

Nano-Sized Adsorbent from Pyrolysed Sago Activated Sludge for Removal of Pb(II) from Aqueous Solution

Nur Aqilah Makshut, Zainab Ngaini*, Rafeah Wahi*, Hasnain Hussain, Nurul Iwani Mahmut and Nurul Qhalila Bahrin

Faculty of Resource Science and Technology, Universiti Malaysia Sarawak, 94300 UNIMAS, Kota Samarahan, Sarawak, Malaysia

ABSTRACT

Increased disposal of heavy metals, including lead (II) (Pb(II)) into the environment calls for a reliable and sustainable solution. In this study, nano-sized biochar from sago activated sludge was proposed for the removal of Pb(II). Sago activated sludge was pyrolysed in a tube furnace followed by a chemical activation to yield nano-sized particles ranging from 45 to 75 nm. The nano-sized biochar obtained was characterised and the influence of pH (2 – 10), initial Pb(II) concentration (1 – 5 mg/L), contact time (30 – 90 mins) and adsorbent dosage (0.1 – 0.5 g) was investigated in a batch adsorption study. Response surface methodology (RSM) approach with central composite design (CCD) was used as statistical tools to optimize the adsorption process by relating the mutual interactions among all studied variables. Characterisation of the prepared adsorbent showed that large surface area was observed on sludge activated carbon (78.863 m²/g) compared with sludge biochar (8.044 m²/g) and sludge biomass (1.303 m²/g). The batch adsorption best fitted the Langmuir isotherm (maximum adsorption capacity, $Q_0 = 3.202 \times 10^{-3}$ mg/g, R-squared value = 0.9308). The RSM indicated that the optimum Pb(II) removal (99.87%) was at 0.5 g of adsorbent, 5 mg/L initial concentration and 30 min contact time. This study is significant because utilisation of sago effluent will reduce sago manufacturing waste by conversion into a value-added product as adsorbent to adsorb Pb(II) in wastewater.

ARTICLE INFO

Article history:

Received: 10 February 2020

Accepted: 14 April 2020

Published: 16 July 2020

E-mail addresses:

aqilahmakshut@gmail.com (Nur Aqilah Makshut)

nzainab@unimas.my (Zainab Ngaini)

wrafeah@unimas.my (Rafeah Wahi)

hhasnain@unimas.my (Hasnain Hussain)

nuruliwani.ni@gmail.com (Nurul Iwani Mahmut)

qnorule@yahoo.com (Nurul Qhalila Bahrin)

* Corresponding author

Keywords: Activated carbon, adsorption, nano-sized adsorbent, RSM, sago, tube furnace

INTRODUCTION

Heavy metal pollution into the aquatic environment including lead (Pb) could cause adverse effects to aquatic habitats as well as humans, resulting in severe mucous irritation, widespread capillaries damage and central nervous system irritation (Ahmad et al., 2009). For example, Pb(II) is refractory and not biologically detoxifiable, and tends to bioaccumulate over time. It may be introduced into water bodies from various sources, such as storage batteries, lead smelting, plating ammunition, ceramic glass industries and tetraethyl lead manufacturing industries (Ahmad et al., 2009).

Many technologies have been introduced to remove Pb(II) in the water, such as physical treatment including coagulation/flocculation and chemical treatment namely chemical precipitation, and ion-exchange and electrochemical process (Amuda et al., 2007). However, there are limitations using these technologies in terms of the treatment cost and effectiveness in removing heavy metals, especially at lower concentrations (Amuda et al., 2007).

Biosorption is commonly reported in the treatment of heavy metals in the wastewater due to its effectiveness and low treatment cost (Ahmad et al., 2009). Biosorption utilizes the ability of a natural sorbent such as agricultural wastes to accumulate heavy metal ions in the aqueous solution by metabolically mediated or physicochemical pathways of uptake (Abbas et al., 2014). There are several biosorbents reported from agricultural wastes such as banana peels (Anwar et al., 2010), palm oil empty fruit bunch (Wahi et al., 2009), sawdust of *Pinus sylvestris* (Taty-Costodes et al., 2003), and Nigerian bamboo (Ademiluyi & Nze, 2016) for the removal of heavy metals from the wastewater. Sludge-based biosorbent was reported to have better average pore diameter (5.62 nm) and mesopore range of 3.13-5.70 nm with higher materials uptake up to 99.7% (Wang et al., 2008; Aliakbari et al., 2016). The utilisation of sludge-based activated carbon for nutrient removal (Yue et al., 2018) or other value-added products such as spirulina cultivation in sago starch factory (Phang et al., 2000) is able to improve waste management in Malaysia in terms of waste disposal cost reduction (Aliakbar et al., 2016).

Sago industry in Malaysia has produced an abundance of agricultural wastes during starch production, which offering potential alternative low-cost materials as biosorbents for the removal of heavy metals such as Pb(II). Approximately 10 – 22 tonnes of sago effluent is generated daily and considered massive compared to the other wastes such as *hampas* and bark which can be reused as value-added products (Ngaini et al., 2013; Wahi et al., 2017a; Ngaini et al., 2014a; Ngaini et al., 2014b; Ngaini et al., 2018). Sago effluent contains high organic content, high biological oxygen demand (BOD), chemical oxygen demand (COD) and other nutrients (Ngaini et al., 2014a) and can be treated *via* the activated sludge process. These benefits meet the suitability of sago effluent to be treated *via* the activated sludge process.

Agricultural waste such as sago activated sludge is a potential feasible and sustainable feedstock for large scale production of nanoparticles for adsorbent purpose. Nanoparticles play a vital role in water treatment, attributing to its excellent properties including small and uniform particle size, high surface area, and composition distribution (Tara et al., 2020). There were limited studies reported on the use of agricultural waste as a source of nanoparticles, and none on sago activated sludge use as nano-sized adsorbent.

Determination and optimization of the nano-sized adsorbent can be done by utilizing the Response Surface Methodology (RSM). It is a statistical method to optimize a certain process by relating the mutual interactions among all variables and providing an estimation of the joined impact of these variables on the results (Kishnor et al., 2006). In addition, a second-order Central Composite Design (CCD) is used to determine and evaluate the optimum variables on the adsorption efficiency. In other words, CCD is used to optimise the parameters with reduced number of experiments while analysing the interactions among parameters (Tan et al., 2008). The analysis of interactions between parameters might take longer time and more experimental runs if the batch adsorption method was applied. Thus, utilising RSM in CCD can improve time and cost management.

In this work, we reported a novel nano-sized adsorbent synthesized from sago activated sludge via pyrolysis and chemical activation method. The physicochemical characterisation, morphology and surface area were characterised, and the adsorptive capability for Pb(II) removal was studied *via* batch adsorption study and optimization of Pb(II) removal was studied using response surface methodology (RSM) approach.

METHODS

Preparation of Sludge Activated Carbon (SAC)

Sago effluent was collected in 20 L tanks from Herdson Sago Industries, Sarawak. Urea (24 g) and phosphoric acid (200 mL) were added into the effluent (20 L) with carbon (C), nitrogen (N), and phosphorus (P) at C:N:P ratio of 100:10:1 (Winkler, 2013). The effluent was aerated for 7 days, filtered and sun-dried to obtain 93.2 g of sludge biomass (SBS). SBS (5 g) was sieved (45 μ m) and heated using a tube furnace (1200 Mini Tube Furnace TI-01200-50SL) under N₂ atmosphere at 400°C for 30 min to yield sludge biochar (SBC) (3 g). SBC (3 g) was soaked in NaOH (5 M, 30 mL) for 2 hr. The mixture was filtered and washed to pH 7. The solid was oven-dried at 100°C for 24 hr for further pyrolysis at 500°C for 90 mins. The carbon was treated with HCl (5 M, 5 mL) to remove impregnating salt and washed using distilled water (150 mL) until pH 4. The solid obtained was oven-dried at 100°C for 1 hr to get 2.8 g of SAC and stored in a desiccator for further usage.

Physicochemical Characterisation

Assessment of Water Quality after Activated Sludge Process. The assessment of water quality was carried out based on the pH, Chemical Oxygen Demand (COD), Total Suspended Solids (TSS), ammoniacal nitrogen (AN). The pH of sago effluent was measured using a pH meter and performed in triplicates, where average values were taken.

Determination of Chemical Oxygen Demand (COD). A COD reactor was turned on to reach a thermal temperature of 150°C. About 2 mL of sago effluent were pipetted into a COD vial which contained COD reagent and inverted three times. A blank sample was prepared using 2 mL of deionized water, heated for 2 h and placed on the HACH instrument. The sample of sago effluent was then placed into the holder for COD analysis (Romes, 2009). The COD analyses were performed in triplicates where average values were taken.

Determination of Total Suspended Solids (TSS). A membrane filter (0.45 µm, 47 mm, white grid) was cleaned and weighed. About 300 mL of the water sample was filtered and the filter was dried in the oven at 100°C for 1 h, cooled to room temperature and weighed. The procedures were repeated in triplicates until a constant weight was obtained. The calculation for TSS is shown in Equation 1:

$$\text{Total Suspended Solids, mg/L} = (A - B) \text{ mg} / (C/1000) \text{ L} \quad [1]$$

where A is weight of filter + residue (mg), B is weight of filter (mg) and C is volume of filtered sample (L).

Determination of Ammoniacal Nitrogen (AN). Nessler method ranging from 0 to 2.5 mg/L was used for NH₃-N analysis. Two Falcon tubes were filled with 25 mL of water sample and deionised water as a blank. Three drops of polyvinyl alcohol as mineral stabiliser were added dropwise into each falcon tube. About 1.0 mL of Nessler reagent was pipetted into each falcon tube. The blank and sample mixture were placed on the HACH instrument to obtain the value of NH₃-N (Romes, 2009). The AN analysis was performed in triplicates where average values were taken.

Proximate Analysis

The procedure for obtaining the moisture content, volatile matter content, ash content and fixed carbon content of SBS, SBC and SAC was adapted from American Society for Testing Materials (ASTM) D-3173, D-3175 and D-3174, respectively.

Moisture Content. Empty, dried crucible (W_e) was weighed. A certain amount of samples was added into the crucible, weighed and labelled (W_s). The sample was dried at 105°C for 24 h. The sample was dried until a constant weight was obtained. The dried sample was weighed again and denoted as W_d . The moisture content of samples was calculated by using Equation 2:

$$\text{Moisture Content (\%)} = \frac{W_s - W_d}{W_s - W_e} \times 100 \% \quad [2]$$

Volatile Matter. Empty dried crucible (W_e) was weighed. A certain quantity of samples was placed into the crucibles, weighed and labelled (W_s). The sample was dried for 7 mins in a furnace at 500°C . The dried sample was then weighed and denoted as W_v . The volatile matter content of samples was calculated by using Equation 3:

$$\text{Volatile Matter Content (\%)} = \frac{W_s - W_v}{W_s - W_e} \times 100 \quad [3]$$

Ash Content. Empty dried crucible was weighed (W_e). The sample was kept dry for 24 hr in a desiccator before the ashing process. The dried sample was placed into the crucible and weighed (W_s). The sample was burnt in a furnace for 3 hr with the first 1 hr at 500°C and the subsequent 2 hr at 700°C . The crucible with the dried sample was labelled (W_a). The ash content was calculated by using Equation 4:

$$\text{Ash Content (\%)} = \frac{W_s - W_a}{W_s - W_e} \times 100\% \quad [4]$$

Fixed Carbon. The fixed carbon content in samples was calculated by using Equation 5:

$$\text{Fixed Carbon (\%)} = (\% \text{ moisture content} + \% \text{ volatile matter} + \% \text{ ash content}) \quad [5]$$

Instrumental Analysis

The characterisation of the functional groups' presence in SBS, SBC and SAC was conducted by using Fourier transform infrared spectroscopy (FTIR) (Thermo Scientific Nicolet IS10 FTIR Spectrometer). Approximately 2 mg of sample in 400 mg dried KBr powder were compressed into a pellet and analysed. The IR spectra were plotted over a frequency range from $400 - 4000 \text{ cm}^{-1}$. The surface morphology and the size of particles were analysed using Transmission Electron Microscope (TEM) (JEOL 1230 Electron Microscope) with magnification 100,000x. The specific surface area was determined using Brunauer-Emmett-Teller (BET) (Quantachrome ASIQC0000-3) with liquid nitrogen adsorption at 77 K.

Batch Adsorption of Pb(II)

Effect of pH on the Adsorption of Pb(II). Pb(II) solution (5 mg/L) was prepared in a 100 mL distilled water. The adsorption was carried out at room temperature with adsorbent dosage 0.5 g. The solution was adjusted to pH 2 – 10 by using HCl (1 M) and NaOH (1 M). The mixture was agitated at 260 rpm for 30 min (Bishnoi et al., 2004). The adsorbent was filtered and analysed using Inductively Coupled Plasma-Optical Emission Spectroscopy (ICP-OES) (Perkin Elmer Optima 8000) (Kumar & Kirtika, 2009).

Effect of Adsorbent Dosage on the Adsorption of Pb(II). Pb(II) solution (5 mg/L) was prepared in a 100 mL distilled water. The adsorption was carried out at room temperature with adsorbent dosage ranging from 0.1 to 0.5 g. The solution was adjusted to pH 8 by using NaOH (1 M). The mixture was agitated at 260 rpm for 30 min (Bishnoi et al., 2004). The adsorbent was filtered and analysed using ICP-OES.

Effect of Initial Concentration on the Adsorption of Pb(II). Pb(II) solution in various concentrations (1 – 5 mg/L) was prepared in a 100 mL distilled water. The experiment was conducted at room temperature. The solution was adjusted to pH 8 by using NaOH (1 M). The adsorbent dosage (0.5 g) was used and agitated at 260 rpm for 30 min. The adsorbent was filtered and analysed using ICP-OES.

Adsorption Isotherms

Adsorption isotherm was used to determine the adsorption characteristic of Pb(II) on SAC. Two types of isotherm model were studied, the Langmuir isotherm and Freundlich isotherm. The Langmuir isotherm was calculated using Equation 6.

$$\text{Langmuir isotherm: } \frac{C_e}{q_e} = \frac{1}{Q_{ob}} + \frac{C_e}{Q_0} \quad [6]$$

where C_e is the equilibrium concentration of Pb(II) after adsorption and q_e , mg/g is the amount of Pb(II) adsorbed per unit mass of adsorbent at equilibrium. The Q_0 (theoretical maximum adsorption capacity (mg/g)) and b (Langmuir adsorption constant (L/mg)) were obtained from the slopes and intercepts of linear plot of (C_e/q_e) versus C_e , respectively (Desta, 2013).

The separation factor or equilibrium parameter (R_L) is essential to predict the affinity between sorbate and sorbent using a separation factor in order to support that the adsorption fits the Langmuir Isotherm (Desta, 2013). R_L can be calculated via Equation 7:

$$\text{Equilibrium parameter: } R_L = \frac{1}{(1 + bC_i)} \quad [7]$$

where b is Langmuir constant (L/mg) obtained from the plotted graph C_e/q_e against C_e . C_i is the initial concentration of Pb(II) solution in mg/L. The adsorption is deduced as irreversible when the $R_L = 0$, linear when $R_L = 1$, unfavourable when $R_L > 1$ or favourable when $0 < R_L < 1$ (Desta, 2013).

The Freundlich isotherm was calculated by using Equation 8.

$$\text{Freundlich isotherm: } \log q_e = \log K_f + \frac{1}{n} \log C_e \quad [8]$$

where, q_e is the amount of Pb(II) adsorbed per unit mass of adsorbent at equilibrium. The K_f is a constant indicative of the adsorption capacity of the adsorbent. The n is an empirical constant connected to the magnitude of the adsorption driving force. The constant value Freundlich, K_f and n were obtained from the graph of $\log q_e$ against $\log C_e$ (Kanawade & Gaikwad, 2011).

Response Surface Methodology (RSM)

The operating variables chosen for RSM in CCD study by using SAC as adsorbent were the adsorbent dosage, initial concentration and contact time. The initial concentration was set from 1 to 5 mg/L. The contact time range was 30 – 90 mins while the adsorbent dosage used ranged from 0.1 to 0.5 g for 50 mL Pb(II) solution volume. The pH of the solution (pH 2) and temperature (STP) were kept constant throughout the experiments. The output parameter was the efficiency of Pb(II) removal in percentage. There were 17 experimental standards generated from Design Expert 7.1.6 (trial version) based on the variable values.

RESULTS AND DISCUSSION

Physicochemical Characterisation

During the aeration process for preparing the SAC, oxygen supply was introduced to the microorganism present in the effluent. The microbes utilized the dissolved oxygen and transformed wastes into more biomass and carbon dioxide (Carrier et al., 2012). Additional nutrients such as phosphorus and urea in the tank were able to provide more nutrients for the microorganisms to grow and clump together (Winkler, 2013). Nitrogen from urea plays an important role in the production of biomass from the activated sludge process. Limited amount of nitrogen influences the filamentous growth, which leads to poor settling process

(Slade et al., 2011). Micronutrients present in the effluent promote higher percentage of methane and carbon dioxide instead of additional biosolids (Amuda et al., 2008).

Pyrolysis of SBS to SBC in the tube furnace at 400°C gave a total carbonisation percentage of 56.4%. High temperature during pyrolysis promotes volatilisation and produces char with a high value of fixed carbon and porosity (Wahi et al., 2017b). The porosity of biochar plays an important factor for excellent adsorption. Sodium hydroxide (NaOH) was used during the activation to produce more porous surfaces (Foo & Hameed, 2012a) and improve sorption properties (Park et al., 2013). NaOH is commonly used as it is cheaper, less corrosive and more environmentally friendly compared with other activating agents such as KOH, ZnCl₂, and H₃PO₄ (Perrin et al., 2005).

Assessment of Water Quality after Activated Sludge Process

The water assessment for pH, chemical oxygen demand (COD), total suspended solids (TSS) and ammoniacal nitrogen (AN) was conducted on sago effluent before and after the activated sludge process. The pH of effluent was improved from pH 4 to pH 7. The COD of sago effluent showed a sharp decrease after the activated sludge process from 30.0±0.33 mg/L to 16.67±0.17 mg/L. Reducing 50% of the values indicated better improvement in water quality after the sludge process (Gerardi, 2002). TSS in sago effluent also decreased from 176.6±0.65 mg/L to 153.3±0.54 mg/L. High suspended solids in a water body could block sunlight from penetrating the water and preventing photosynthesis of aquatic plants to occur (Gerardi, 2002). AN also showed reduced amount from 21.0±0.16 mg/L to 0.71±0.55 mg/L. The summary of results for the water assessments can be observed in Table 1.

Table 1
Water assessment on sago effluent before and after the activated sludge process

Assessment	Before process	After process
pH	4	7
COD (mg/L)	30.0±0.33	16.67±0.17
TSS (mg/L)	176.6±0.65	153.3±0.54
AN (mg/L)	21.0±0.16	0.71±0.55

Proximate Analysis. Proximate analysis of SBC and SAC is tabulated in Table 2. The moisture content of SBC reduced from 0.514% to 0.0% after pyrolysis at 500°C, indicating complete removal of volatile matter (Wahi et al., 2017b). SAC yielded low moisture content compared to SBC due to carbonization process, which caused the loss of volatile matter (Rafiq et al., 2016). The longer heating period of biochar is essential to improve the quality and lower moisture content of activated carbon (SAC) (Wahi & Senghie, 2010). A less volatile matter that clogged the pores of biochar caused a decrease in the percentage

of the volatile matter of SBC (0.084%) and SAC (0.001%) (Wahi et al., 2017b). High carbonization temperature released a high amount of volatile matter from breaking of weaker bridges and bonds in organic matrices (Qian et al., 2008).

Ash content in SAC was improved to 99.9% from 99.1% in SBC which indicated that inorganic residue was higher in SAC (Rafiq et al., 2016). The ash content shows a significant increase as the ash remains in the solid fraction whereas the organic matter undergoes thermal decomposition, resulting in the decrease of the fixed carbon content in SBC from 0.30% to 0.08% in SAC (Ronsse et al., 2012).

Table 2

Proximate analysis of SBC and SAC

Proximate analysis	SBC	SAC
Moisture content, %	0.514	0
Volatile matter, %	0.084	0.001
Ash content, %	99.1	99.9
Fixed carbon content, %	0.30	0.08

Instrumental Analysis

Functional Group Analysis. The FTIR spectra of SBS, SBC and SAC are shown in Figure 1. The adsorption peaking at 3408 – 3426 cm^{-1} was attributed to the $\nu_{\text{O-H}}$ stretching vibration of carboxylic acids, phenols and alcohols in lignin, cellulose and pectin present

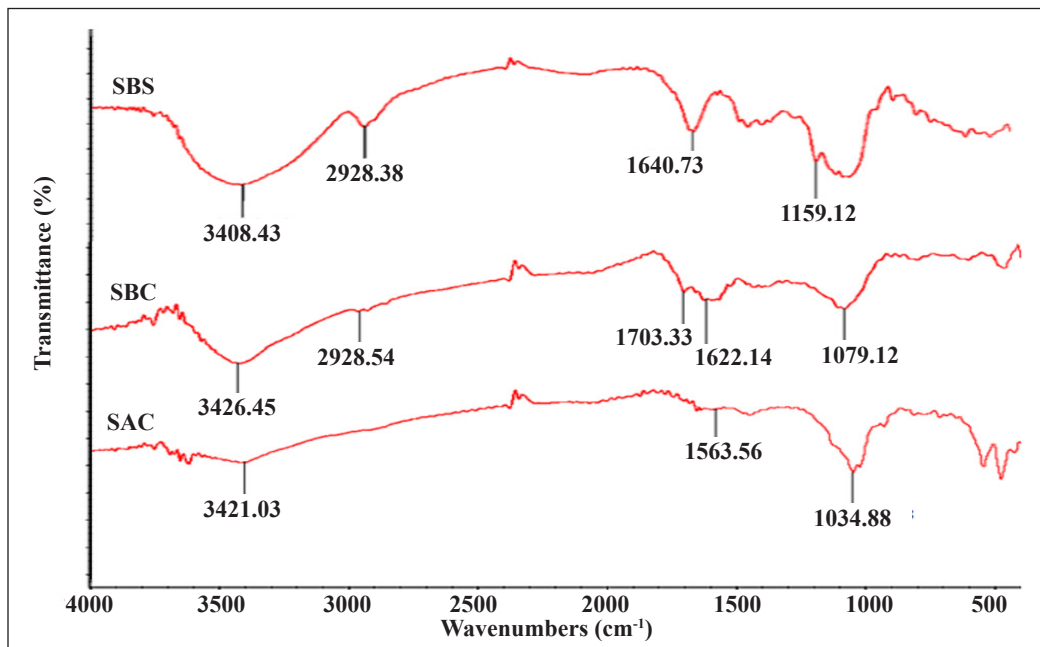


Figure 1. IR Spectra of (a) SBS, (b) SBC and (c) SAC

in SBS (Pathania et al., 2017). The broad O-H peak in SBS (Figure 1a) was reduced after the double carbonisation and activation process (Figure 1b-c). The pyrolysis caused the decomposition of functional groups and liberation of volatile matter during carbonisation (Foo & Hameed, 2012a). A weak peak at 2928 cm^{-1} corresponded to $\nu_{\text{C-H}}$ ($-\text{CH}_2$, $-\text{CH}_3$) was observed in SBS and reduced in SBC and SAC after pyrolysis. The peaks at 1622 - 1703 cm^{-1} could be due to the stretching vibration of $\nu_{\text{C=C}}$ and $\nu_{\text{C=O}}$ from lignin and hemicellulose in SBS and SBC and reduced after activation in SAC (Tan et al., 2008). The appearance of strong peaks in the spectra at 1034 - 1079 cm^{-1} was assigned to $\nu_{\text{C-N}}$ presence in the samples (Stella et al., 2016).

Transmission Electron Microscope (TEM) Analysis. The TEM image of SAC is shown in Figure 2. The pyrolysis of SBS at 400°C in the tube furnace under inert nitrogen atmosphere followed by chemical activations produced spherical, nano-sized particles within the range of 45 - 75 nm . The high temperature of a fast pyrolysis or carbonisation reaction in the tube furnace reduced the size of particles into nano-sized particles (Hedge et al., 2015). The size of carbon particles plays an important role in the adsorption capacity of a composite. Small-sized adsorbent provides a larger surface area which increases the rate of effective collision, increasing the binding probability between sorbent and sorbate, thus increasing the adsorption. The carbon particle size of composite with range 75 - $150\text{ }\mu\text{m}$ was reported to give higher adsorption capacity than that of 850 - $1000\text{ }\mu\text{m}$ (McKay, 1982). Similarly, effective adsorption of heavy metals was reported on carbon with a diameter range of 0.25 - 0.5 mm or lower, and ineffective with diameter $>1.25\text{ mm}$ (Ricordel et al., 2001). The higher uptake by smaller particles is due to greater accessibility to pores and larger surface area for mass adsorption per unit weight of carbon (Senthilkumar et al., 2005).

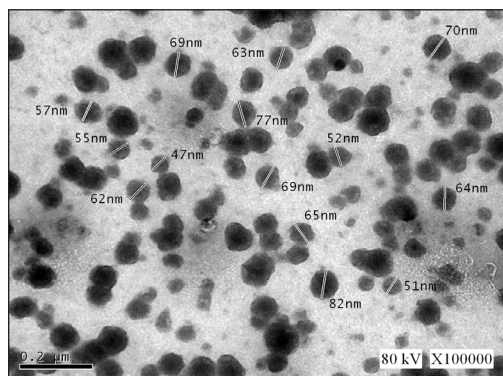


Figure 2. TEM image of SAC

Brunauer Emmett and Teller (BET) Analysis. The surface area of SBS ($1.303\text{ m}^2/\text{g}$) was characterised using BET. The surface area increased after pyrolysis from $8.044\text{ m}^2/\text{g}$ (SBS) to $78.863\text{ m}^2/\text{g}$ (SAC). The results showed a highly significant surface area difference between untreated and treated biochar. The large surface area of SAC was due to the larger pore size of SAC (Rajan et al., 2019). The surface area of SAC is highly dependent on the carbonization temperature with a higher temperature giving larger surface areas (Hu & Srinivasan, 1999). Double physical activation followed by chemical treatment with NaOH

aids in the production of a larger surface area of SAC. The large surface area was due to the intercalation of the carbonate metal from NaOH to the carbon matrix, thus broadening the space between the carbons' atomic layer (Foo & Hameed, 2012b).

Batch Adsorption of Pb(II)

Effect of pH on the Adsorption of Pb(II). The pH of the aqueous suspension of an adsorbent is a crucial factor that controls the adsorption of heavy metals (Gaya et al., 2015). From Figure 3, the highest adsorption occurred at pH 8 (95.06%) while the lowest was at pH 2 (12%). This is plausibly due to at lower pH (<pH 8), the presence of H⁺ ions reduces the interaction with the predominant Pb(II) species (El-Ashtouky et al., 2008). The adsorption reached equilibrium at pH 8 and decreased at pH 10 due to the negatively charged surface of activated carbon sludge. Soluble hydroxylated complexes were also formed at higher pH, causing competition between the complexes and Pb ions for the binding sites (Ibrahim et al., 2016).

Effect of Adsorbent Dosage on the Adsorption of Pb(II). In this study, a series of batch adsorption experiment was performed to investigate the effect of adsorbent dosage (0.1 – 0.5 g) employing SAC for the adsorption of Pb(II). The activated carbon sludge demonstrated excellent removal efficiency with the increased removal of Pb(II) from 27.4 to 99.78% as the adsorbent dosage increased from 0.1 – 0.5 g. The removal efficiency is commonly corresponding to the surface area and particle size of the adsorbent. Effective adsorption of heavy metals on carbon with a diameter range of 0.25 – 0.5 mm or lower (Ricordel et al., 2001) gave higher uptake due to greater accessibility to pores and larger surface area for mass adsorption per unit weight of carbon (Senthilkumar et al., 2005). High surface area (78.863 m²/g) of SAC contributed to the excellent adsorption capacity of Pb(II) (McKay,

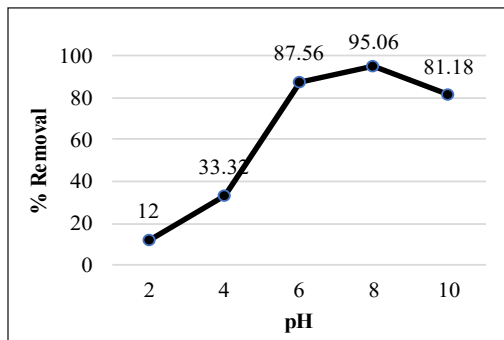


Figure 3. Effect of pH on the Adsorption of Pb(II) (Experimental conditions: Pb(II) concentration: 5 mg/L, adsorbent dosage: 0.5 g/100 mL (0.005 g/mL), adsorption time: 30 min, mixing rate: 260 rpm, pH: 8)

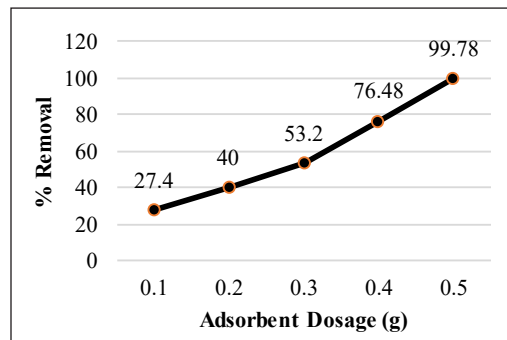


Figure 4. Effect of Adsorbent Dosage on the Adsorption of Pb(II) (Experimental conditions: Pb(II) concentration: 5 mg/L, adsorption time: 30 min, mixing rate: 260 rpm, pH: 8)

1982), with advantage on its nanosize particles (Figure 2). Overall, the percentage of removal increased with the increase in dosage of adsorbent (0.1–0.5 g) (Figure 4). This is due to the higher exchangeable site and surface areas of the adsorbent, which leads to better adsorption capacity (Patil et al., 2011; Gao et al., 2013).

Effect of Initial Concentration on the Adsorption of Pb(II).

The adsorption of Pb(II) decreased from 84.18 to 27.18% as the initial concentration of Pb(II) decreased from 1 to 5 mg/L (Figure 5). This trend suggested for the possible monolayer adsorption (Hu et al., 2009) of Pb(II) onto the surface of SAC. At higher concentration, the mass transfer of Pb(II) molecules becomes limited as the availability of binding sites is very low (Mehdizadeh et al., 2014). In fact, initial concentration is an important parameter to promote a driving force and improve mass transfer resistance from aqueous to solid phases adsorbent (Hema & Srinivasan, 2010).

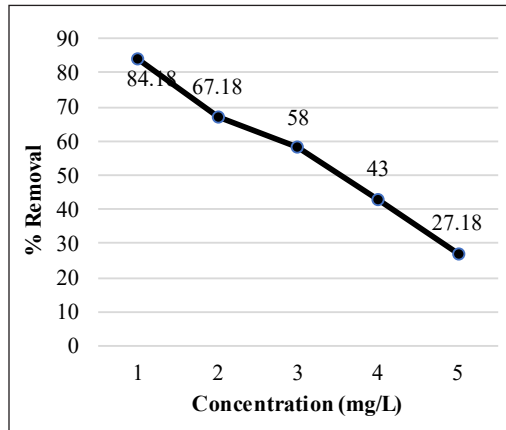


Figure 5. Effect of Initial Concentration on the Adsorption of Pb(II) (Experimental conditions: Pb(II) concentration: 1-5 mg/L, adsorbent dosage: 0.5 g/100 mL (0.005 g/mL), adsorption time: 30 min, mixing rate: 260 rpm, pH: 8)

Adsorption Isotherms

Langmuir Isotherm. The graph of (Ce/qe) against Ce (Figure 6) demonstrated that the experimental data of Pb(II) ions removal by SAC fitted well with Langmuir isotherm (R²=0.9308), indicating a monolayer adsorption. Langmuir isotherm model proposes a good sorption method of monolayer adsorption on a homogenous adsorbent layer, without any interaction between the adsorbate molecules and adjacent sites (Fat’hi et al., 2014). Table 3 shows that the constant b showed high adsorption energy (0.5108 L/mg), indicating a fast increment in adsorption at low concentrations of adsorbate (Mor et al., 2006).

The maximum adsorption capacity, Q₀ obtained from Langmuir isotherm for removal of Pb(II) by SAC in comparison with other adsorbents is depicted in Table 3.

Table 3
Equilibrium constant of Langmuir Isotherm and Freundlich Isotherm on the removal of Pb(II)

Isotherm	Parameters	Values
Langmuir	Q ₀ (mg/g)	3.202 × 10 ⁻³
	b (L/mg)	0.5108
	R ²	0.9308
	R _L	0.999
Freundlich	n	2.5109
	1/n	0.399
	K _f	1.131 × 10 ⁻³
	R ²	0.9084

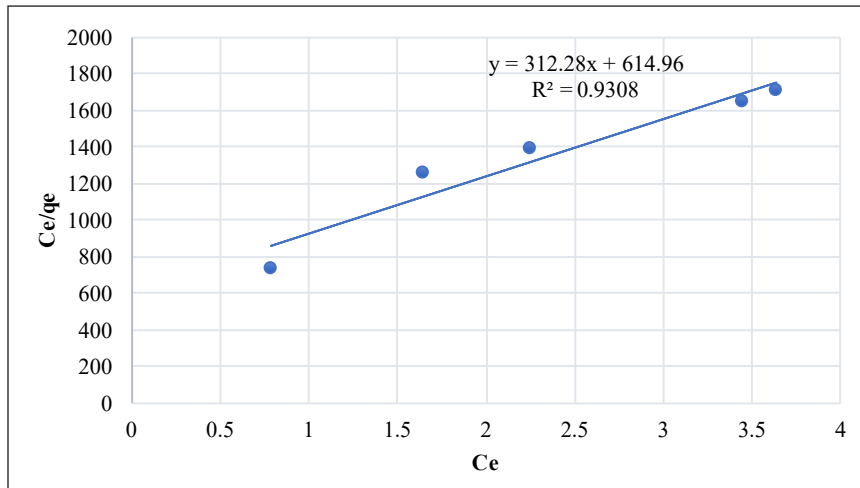


Figure 6. Langmuir isotherm plot for Pb(II) adsorption by SAC (Experimental conditions: Pb(II) concentration: 1-5 mg/L, adsorbent dosage: 0.5 g/100 mL (0.005 g/mL), adsorption time: 30 min, mixing rate: 260 rpm, pH: 8)

The SAC had relatively low adsorption capacity (3.202×10^{-3}) compared to other adsorbents from previous studies. Most of the studies however, were conducted at acidic pH, and higher Pb(II) concentration compared to the present study. One of the plausible reason for the low adsorption capacity of SAC is the adsorption condition, which was conducted at basic pH (pH 8). Previous studies as shown in Table 4 showed that maximum removal of Pb(II) ions is observed at pH 5.6–7.6. At a higher pH, Pb(II) ions form hydroxide precipitate, which consequently decreases the adsorption rate and removal percentage (El-Ashtoukhy et al., 2008). On the other hand, batch adsorption experiments in the present study shows high removal of Pb(II) (maximum removal 99.78%) despite of the low Q_0 value. The high removal percentage might be attributed to the high adsorbent dosage (0.02 g/mL) used for removal of Pb(II) at very low initial concentrations (1-5 mg/L). At high adsorbent dosage more active sites are available for metal uptake (Anwar et al., 2010).

Freundlich Isotherm. Freundlich isotherm for Pb(II) adsorption by SAC is shown in Figure 7 and the corresponding parameters are shown in Table 3. The adsorption intensity, n was 2.51 ($n > 1$). The n value showed the degree of non-linearity between the solution concentration and adsorption. Should the value of n is 1, the adsorption is assumed as linear. If $n < 1$, the adsorption is a chemical process while $n > 1$ is the most common degree on non-linearity obtained due to the distribution of surface sites that causes a decrease in adsorbent-adsorbate interactions as surface density is increasing (Reed & Matsumoto, 1993).

The $1/n$ value of SAC was 0.399 (Table 3), indicates a normal Langmuir isotherm ($1/n < 1$) (Fan et al., 2013) with only a slight intensity of heterogenous layer adsorption

Table 4
 Comparison on maximum adsorption capacity, Q_0 obtained from Langmuir isotherm for removal of Pb(II) by different adsorbent

	Adsorbent	Q_0 , mg/g	Adsorption condition	Author(s)
(i)	Banana peels	2.18	Pb(II) concentration: 30-80 mg/L Adsorbent dosage: 40 g/L (0.04 g/mL) Adsorption time: 20 min Mixing rate: 100 rpm pH: 5	Anwar et al. (2010)
(ii)	Tamarind wood activated carbon	43.85	Pb(II) concentration: 10-50 mg/L Adsorbent dosage: 2 g/L (0.002 g/mL) Adsorption time: 30 min Mixing rate: 120 rpm pH: 6.5	Acharya et al. (2009)
(iii)	Mesembryanthemum activated carbon	66.67	Pb(II) concentration: 50-1000 mg/L Adsorbent dosage: 1 g/50 mL (0.02 g/mL) Adsorption time: 24 h Mixing rate: 150 rpm pH: 5	Alkherraz et al. (2020)
(iv)	Urea Treated <i>Leucaena leucocephala</i> Leaf	90.09	Pb(II) concentration: 50-250 mg/L Adsorbent dosage: 0.02 g/50 mL (0.0004 g/mL) Adsorption time: 30 min Mixing rate: 100 rpm pH: 5	Mansur et al. (2020)
(v)	Magnetic chitosan/graphene oxide composites	76.94	Pb(II) concentration: 0.5-14 mg/L Adsorbent dosage: 0.02 g/25 mL (0.0008 g/mL) Adsorption time: 60 min Mixing rate: 180 rpm pH: 5	Fan et al. (2013)
(vi)	Chitosan-tripolyphosphate beads	57.33	Pb(II) concentration: 20-300 mg/L Adsorbent dosage: 0.20 g/50 mL (0.004 g/mL) Adsorption time: 100 min Mixing rate: 400 rpm pH: 4.5	Ngah & Fatinathan (2010)
(vii)	Sago activated carbon (SAC)	3.202×10^{-3}	Pb(II) concentration: 1-5 mg/L Adsorbent dosage: 0.5 g/100 mL (0.005 g/mL) Adsorption time: 30 min Mixing rate: 260 rpm pH: 8	Present study

(Arami-Nya et al., 2012; Tsai et al., 2001). Gao et al. (2013) suggested at $1/n < 1$, adsorption occurred from the interaction between adsorbed molecules with various energies. The ultimate adsorption capacity, K_f was 1.131×10^{-3} , and the R^2 value (0.9084) shows good fitting with Freundlich isotherm.

Both Langmuir and Freundlich isotherms depicted R^2 value larger than 0.900. However, the adsorption of Pb(II) by SAC is best represented by Langmuir isotherm ($R^2=0.9308$).

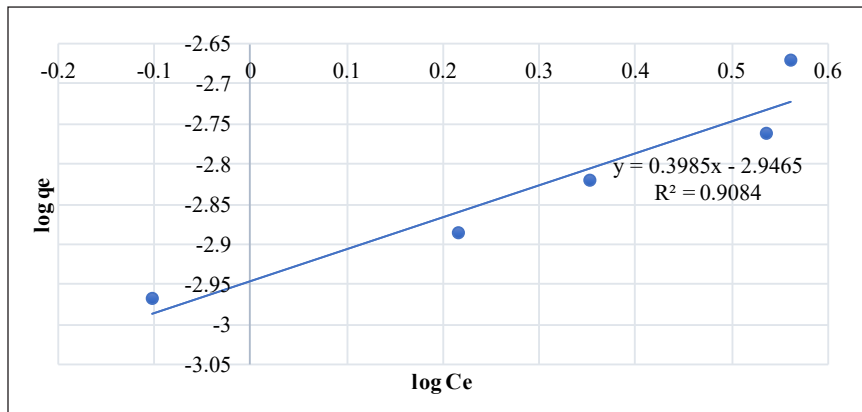


Figure 7. Freundlich isotherm plot for Pb(II) adsorption by SAC (Experimental conditions: Pb(II) concentration: 1-5 mg/L, adsorbent dosage: 0.5 g/100 mL (0.005 g/mL), adsorption time: 30 min, mixing rate: 260 rpm, pH: 8)

The separation factor, R_L obtained was 0.999, indicating that the adsorption of Pb(II) onto SAC was favourable ($0 < R_L < 1$).

Response Surface Methodology (RSM)

Table 5 shows the design matrix, experimental conditions; initial concentration (A), adsorbent dosage (B) and contact time (C), their ranges and responses which are percentage removal of Pb(II) ions by SAC at pH 2, to simulate the strongly acidic nature of real wastewater containing Pb ions from battery manufacturing industry (Arunlertaree et al., 2007). The Pb(II) ions removal by SAC ranged between 22.55% to 99.87%. Run 3 shows the highest percentage removal of Pb(II) ions (99.87%) was at the following experimental conditions: Pb(II) initial concentration (5 mg/L), adsorbent dosage (0.5 g), contact time (30 min). The lowest percentage removal of Pb(II) ions (22.55%) was at the following experimental conditions: Pb(II) initial concentration (5 mg/L), adsorbent dosage (0.1 g), contact time (90 min). Results from RSM study showed a contradicting Pb(II) percentage removal response compared to the batch adsorption study. The inconsistency was plausibly due to the combination effects of the parameters studied, which was in different adsorbent dosage settings in both studies i.e. 0.5 g SAC/100 mL (0.005 g/mL) Pb(II) solution in batch adsorption study, and 0.5 g SAC/50 mL Pb(II) (0.01 g/mL) solution in RSM study. Higher adsorbent dosage per volume of Pb(II) solution in RSM studies provided more active sites for adsorption of Pb(II) to occur on SAC surface (Mehdizadeh et al., 2014).

The development of the polynomial regression equations by the Design Expert software suggested quadratic model for Pb(II) removal as response of SAC usage as adsorbent. The model was selected based on the highest order polynomial where the additional terms are significant, and the model is not aliased (Arami-Nya et al., 2012). The final empirical model in terms of coded factors is represented in Equation 9.

Table 5
The percent removal of Pb(II) for 17 experimental runs

Standard Run	Parameter			% Removal of Pb(II)*
	Initial concentration (mg/L)	Adsorbent dosage (g)	Contact time (min)	
1	1.00	0.10	30.00	57.58
2	5.00	0.10	30.00	36.89
3	1.00	0.50	30.00	98.55
4	5.00	0.50	30.00	99.87
5	1.00	0.10	90.00	64.58
6	5.00	0.10	90.00	22.55
7	1.00	0.50	90.00	83.96
8	5.00	0.50	90.00	64.56
9	3.00	0.30	60.00	52.73
10	3.00	0.30	60.00	52.09
11	1.00	0.30	60.00	60.88
12	5.00	0.30	60.00	41.55
13	3.00	0.10	60.00	30.05
14	3.00	0.50	60.00	70.54
15	3.00	0.30	30.00	99.65
16	3.00	0.30	90.00	84.65
17	3.00	0.30	60.00	59.43

$$\text{Percentage removal of Pb(II)} = +56.11 - 10.01A + 20.58B - 7.22C + 5.58AB - 5.26AC - 5.32BC - 8.75A^2 - 9.67B^2 + 32.18C^2$$

[9]

The coefficients with one variable, initial concentration (A), adsorbent dosage (B) and contact time (C) represent the effect of the factors on the responses of percent removal of Pb(II). The coefficients multiplied between two different variables show the correlation between the two variables and quadratic effect. A positive symbol in front of the terms shows synergistic effect while a negative symbol means antagonistic effect (Chowdhury et al., 2012)

The performance of the model can be concluded by determining the plots of predicted against actual (experimental) percentage removal of Pb(II) (Figure 8). High R² value (0.9999) indicates that the experimental data fitted excellently with the developed model. The predicted R² was 0.9989, which was in a reasonable range with the adjusted R² of 0.9996. A model ratio greater than 4 is needed where the model ratio of 205.459 indicates an adequate signal. Thus, this model can be used to navigate the design space.

The coefficient of variance (CV) value determination is crucial as it shows the ratio between the standard error of estimates with the mean value of the observed response as

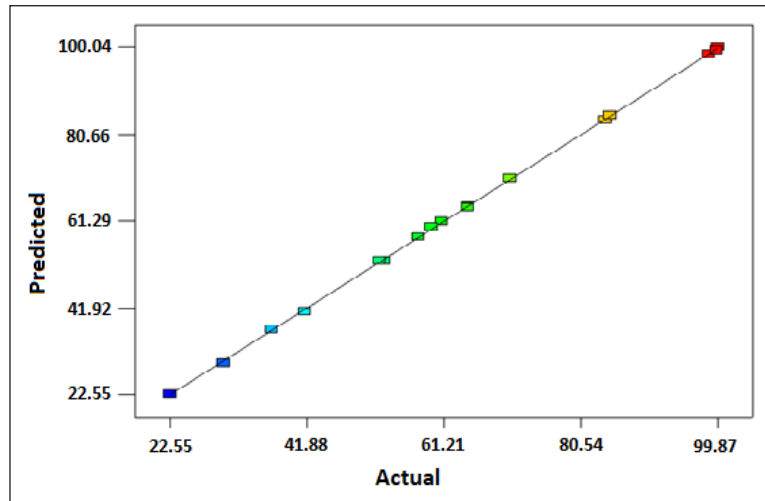


Figure 8. Predicted vs. actual percent removal of Pb(II) using SAC at pH 2 ($R^2 = 0.9999$, Adjusted $R^2 = 0.9996$, Predicted $R^2 = 0.9989$)

a percentage and it measures the reproducibility of the model. The model is considered reasonably reproducible if it is less than 10% (Chowdhury et al., 2012). It was observed that the CV for Pb(II) removal using SAC was 0.73%, indicating a reproducible model.

The 3-dimensional (3D) surface plots for percent removal of Pb(II) based on RSM study are represented in Figure 9. Figure 9 (a), (b) and (c) show the effects of the initial concentration of Pb(II) solution, adsorbent dosage and contact time respectively, on the removal of Pb(II) using SAC at pH 2 and standard room temperature (STP).

Figure 9a shows the effect of the adsorbent dosage and initial concentration on Pb(II) removal. The minimum removal was 36.89% at 0.1 g while the maximum removal was 99.87% at the adsorbent dosage of 0.5 g. The removal of Pb(II) increased as the adsorbent dosage was increased from 0.1 to 0.5 g at a constant concentration of Pb(II) (5 mg/L). At higher adsorbent dosage, more adsorption surfaces are available (Acharya et al., 2009), which subsequently provide more active sites for adsorption to occur (Mehdizadeh et al., 2014).

Figure 9b shows the effect of contact time and initial concentration on the percent removal of Pb(II) when the adsorbent dosage is at a constant (0.1 g). At 90 mins, the highest removal of Pb(II) was 64.68% at 1 mg/L, while the lowest removal of Pb(II) was 22.55% at 5 mg/L. This phenomenon is due to the lower availability of active sites prior to the adsorbent with time, causing limited mass transfer of Pb(II) molecules to the outer surface of adsorbents (Mehdizadeh et al., 2014). The highest removal of Pb(II) in the first 30 min was 57.58% at 1 mg/L while the lowest removal was 36.89% at 5 mg/L. However, at 60 min (3 mg/L), the removal was 30.07%. This phenomenon could be due to the reversibility of the removal process (Ghasemi et al., 2014).

Similar observation was observed on the effect of contact time and adsorbent dosage at the constant concentration of Pb(II) (5 mg/L) (Figure 9c). The maximum removal was 99.87% and slowly reduced to 41.55%, before increasing to 64.56% in 30 – 90 mins. In other words, the shorter time (30 mins) gave the best removal (99.87%) of Pb(II). The removal percentage of Pb(II) in the present study is relatively higher compared to percentage removal of Pb(II) by sawdust of *Pinus sylvestris* (97.6%) (Taty-Costodes et al., 2003) and banana peel (85.3%) (Anwar et al., 2010). The shorter contact time is important for practical wastewater treatment application.

Based on the RSM study, the highest percentage removal of Pb(II) was 99.87% indicating that the optimum conditions of Pb(II) removal was obtained: 0.5 g adsorbent dosage for 50 mL Pb(II) solution, 5 mg/L initial concentration, pH 2 at 30 mins contact time. Acidic condition (pH 2) of the Pb(II) solution may cause SAC fibrous surface to be

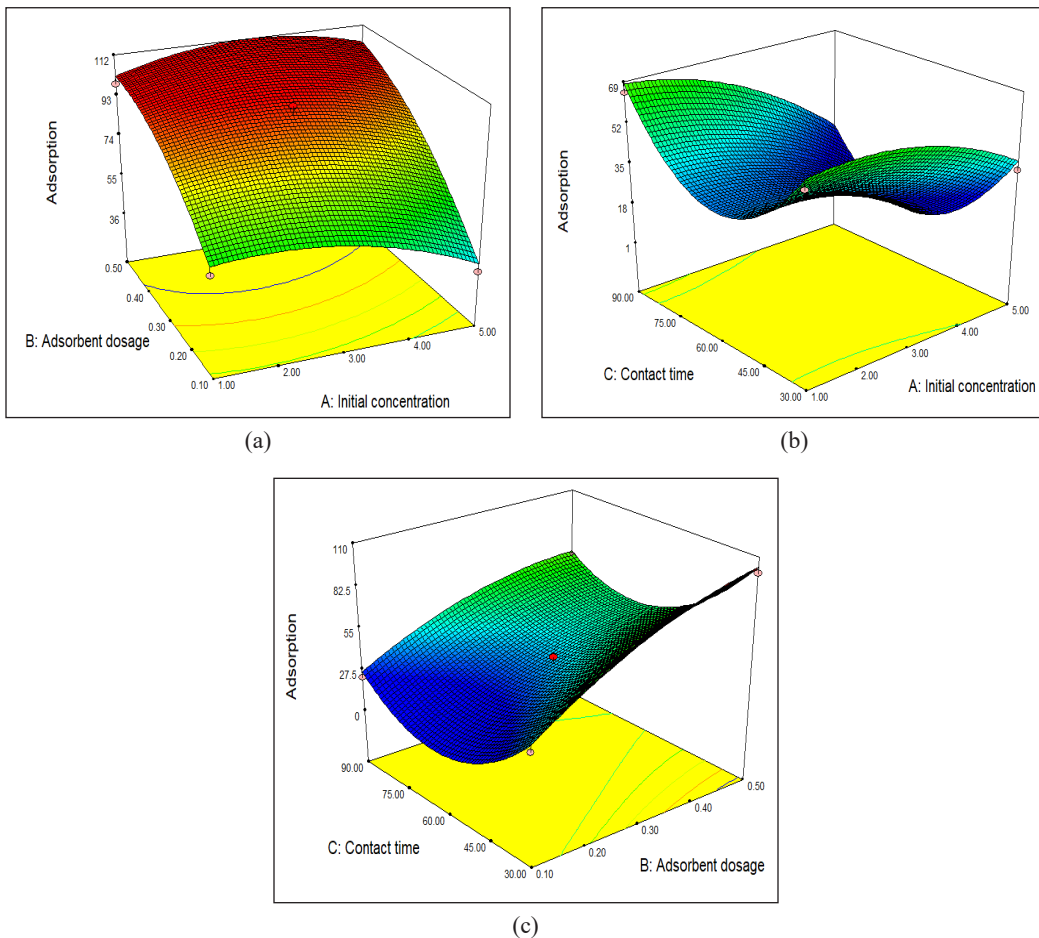


Figure 9. The combined effect of (a) adsorbent dosage and initial concentration with contact time 30 min, (b) contact time and initial concentration with adsorbent dosage 0.1 g, (c) contact time and adsorbent dosage with initial concentration 5 mg/L.

contracted and tightly captured (Arunlertaree et al., 2007), and thus increased the surface area per volume of adsorbent used (Wahi & Senghie, 2010), resulted in an increase of Pb(II) adsorption on SAC surface. In addition, the contact time of 30 min is optimum for maximised adsorption of Pb(II), as shown in previous studies (Taty-Costodes et al., 2003) and banana peel (85.3%) (Anwar et al., 2010)

CONCLUSION

In summary, a spherical nano-sized adsorbent, namely sago activated carbon (SAC) was successfully derived from sago effluent via tube furnace pyrolysis. Characterisation of the prepared adsorbent showed that large surface area was observed on sludge activated carbon (78.863 m²/g) compared with sludge biochar (8.044 m²/g) and sludge biomass (1.303 m²/g). The batch adsorption best fitted the Langmuir isotherm (maximum adsorption capacity, $Q_0 = 3.202 \times 10^{-3}$ mg/g, R-squared value = 0.9308). The RSM indicated that the optimum Pb(II) removal (99.87%) was at 0.5 g of adsorbent, 5 mg/L initial concentration and 30 min contact time. The SAC derived from activated sludge process has the potential to be employed as an adsorbent to reduce the environmental issues related to sago industries.

ACKNOWLEDGEMENTS

The authors would like to thank Universiti Malaysia Sarawak for the research fund (Tun Openg Sago Research Chair: F07/TOC/1742/2018).

REFERENCES

- Abbas, S. H., Ismail, I. M., Mostafa, T. M., & Sulaymon, A. H. (2014). Biosorption of heavy metals: A review. *Journal of Chemical Science and Technology*, 3(4), 74-102.
- Acharya, J., Sahu, J. N., Mohanty, C. R., & Meikap, B. C. (2009). Removal of lead (II) from wastewater by activated carbon developed from tamarind wood by zinc chloride activation. *Chemical Engineering Journal*, 149(1-3), 249-262.
- Ademiluyi, F. T., & Nze, J. C. (2016). Multiple adsorption of heavy metal ions in aqueous solution using activated carbon from Nigerian bamboo. *International Journal of Resource Engineering Technology*, 5(1), 164-169.
- Ahmad, A., Rafatullah, M., Sulaiman, O., Ibrahim, M. H., Chii, Y. Y., & Siddique, B. M. (2009). Removal of Cu(II) and Pb(II) ions from aqueous solutions by adsorption of sawdust of Meranti wood. *Desalination*, 247(1-3), 636-664.
- Aliakbari, Z., Younesi, H., Ghoreyshi, A. A., Bahramifar, N., & Heidari, A. (2016). Production of sewage-sludge based activated carbons under different post-activation conditions. *Waste and Biomass Valorization*, 9(3), 451-463.

- Alkherraz, A. M., Ali, A. K., & Elsherif, K. M. (2020). Equilibrium and thermodynamic studies of Pb(II), Zn(II), Cu(II) and Cd(II) adsorption onto Mesembryanthemum activated carbon. *Journal of Medicinal and Chemical Sciences*, 3(1), 1-10.
- Amuda, O. S., Deng, A., Alade, A. O., & Hung, Y. T. (2008). Conversion of sewage sludge to biosolids. *Biosolids Engineering and Management*, 7, 65-119.
- Amuda, O. S., Giwa, A. A., & Bello, I. A. (2007). Removal of heavy metal from industrial wastewater using modified activated coconut shell carbon. *Biochemical Engineering Journal*, 36(2), 174-181.
- Anwar, J., Shafique, U., Waheed-Uz-Zaman, Salman, M., Dar, A., & Anwar, S. (2010). Removal of Pb(II) and Cd(II) from water by adsorption on peels of banana. *Bioresource Technology*, 101(6), 1752-1755.
- Arami-Nya, A., Daud, W. M. A. W., Mjalli, F. S., Abnisa, F., & Shafeeyan, M. S. (2012). Production of microporous palm shell based activated carbon for methane adsorption: modelling and optimisation using response surface methodology. *Chemical Engineering Research and Design*, 90, 776-784.
- Arunlertaree, C., Kaewsomboon, W., Kumsopa, A., Pokethitiyook, P., & Panyawathanakit, P. (2007). Removal of lead from battery manufacturing wastewater by egg shell. *Songklanakarin Journal of Science and Technology* 29(3), 857-868.
- Bishnoi, N. R., Bajaj, M., Sharma, N., & Gupta, A. (2004). Adsorption of Cr(VI) on activated rice husk carbon and activated alumina. *Bioresource Technology*, 91(3), 305-307.
- Carrier, M., Hardie, A. G., Uras, U., Görgens, J., & Knoetze, J. H. (2012). Production of char from vacuum pyrolysis of south african sugarcane bagasse and its characterisation as activated carbon and biochar. *Journal of Analytical and Applied Pyrolysis*, 96, 24-32.
- Chowdhury, Z. Z., Zain, S. M., Khan, R. A., Arami-Nya, A., & Khalid, K. (2012). Process variables optimization for preparation and characterization of novel adsorbent from lignocellulosic waste. *Bioresources*, 7(3), 3732-3754.
- Desta, B. M. (2013). Batch sorption experiments: Langmuir and freundlich isotherm studies for the adsorption of textile metal ions onto teff straw (*Eragrostis tef*) agricultural waste. *Journal of Thermodynamics*, 2013, 1-7.
- El-Ashtouky, E. S. Z., Amin, N. K., & Abdelwahab, O. (2008). Removal of lead(II) and copper(II) from aqueous solution using pomegranate peel as a new adsorbent. *Desalination*, 223(1-3), 162-173.
- Fan, L., Luo, C., Sun, M., Li, X., & Qiu, H. (2013). Highly selective adsorption of lead ions by water-dispersible magnetic chitosan/graphene oxide composites. *Colloids and Surfaces B: Biointerfaces*, 103, 523-529.
- Fat'hi, M. R., Asfaram, A., Hadipour, A., & Roosta, M. (2014). Kinetics and thermodynamic studies for removal of acid blue 129 from aqueous solution by almond shell. *Journal of Environmental Health Science and Engineering*, 12(1), 62-68.
- Foo, K. Y., & Hameed, B. H. (2012a). Preparation, characterisation and evaluation of adsorptive properties of orange peel based activated carbon via microwave induced K₂CO₃ activation. *Bioresource Technology*, 104, 679-686.
- Foo, K. Y., & Hameed, B. H. (2012b). Potential of jackfruit peel as precursor for activated carbon prepared by microwave induced NaOH activation. *Bioresource Technology*, 112, 143-150.

- Gao, H., Sun, Y., Zhou, J., Xu, R., & Duan, H. (2013). Mussel-inspired synthesis of polydopamine-functionalised graphene hydrogel as reusable adsorbents for water purification. *ACS Applied Materials Interfaces*, 5(2), 425-432.
- Gaya, U. I., Otene, E., & Abdullah, A. H. (2015). Adsorption of aqueous Cd(II) and Pb(II) on activated carbon nanopores prepared by chemical activation of doum palm shell. *SpringerPlus*, 4(1), 1-18.
- Gerardi, M. H. (2002). *Nitrification and denitrification in the activated sludge process*. New York, USA: Marcel Dekker Inc.
- Ghasemi, M., Khosroshahy, M. Z., Abbasabadi, A. B., Ghasemi, N., Javadion, H., & Fattahi, M. (2014). Microwave-assisted functionalisation of *Rosu canina*-L fruits activated carbon with tetraethylenepentamine and its adsorption behaviour towards Ni(II) in aqueous solution: Kinetic equilibrium and thermodynamic study. *Powder Technology*, 274, 362-371.
- Hedge, G., Manaf, S. A. A., Kumat, A., Ali, G. A., Chong, K. F., Ngaini, Z. & Sharma, K. V. (2015). Biowaste sago bark based catalyst free carbon nanospheres: Waste to wealth approach. *ACS Sustainable Chemistry and Engineering*, 3(9), 2247-2253
- Hema, M., & Srinivasan, K. (2010). Uptake of toxic metals from wastewater by activated carbon from ago industrial by-product. *Indian Journal of Engineering and Materials Sciences*, 17(5), 373-389.
- Hu, Z., & Srinivasan, M. P. (1999). Preparation of high-surface-area activated carbons from coconut shell. *Microporous and Mesoporous Materials*, 27(1), 11-18.
- Hu, C., Li, J., Zhou, Y., Li, M., Xue, F., & Li, H. (2009). Enhanced removal of methylene blue from aqueous solution by pummelo peel pretreated with sodium hydroxide. *Journal of Health Science*, 55(4), 619-624.
- Ibrahim, W. M., Hassan, A. F., & Azab, Y. A. (2016). Biosorption of toxic heavy metals from aqueous solution by *Ulva lactuca* activated carbon. *Egyptian Journal of Basic and Applied Sciences*, 3(3), 241-249.
- Kanawade, S. M., & Gaikwad, R. W. (2011). Removal of methylene blue from effluent by using activated carbon and water hyacinth as adsorbent. *International Journal of Chemical Engineering Application*, 2(5), 317-319.
- Kishnor, K., Ujjval, T., & Patel, K. C. (2006). Application of response surface methodology of optimization of lactic acid production using date juice. *Journal of Microbiology and Biotechnology*, 16(9), 1410-1415.
- Kumar, P. S., & Kirtika, K. (2009). Equilibrium and kinetic study of adsorption of nickel from aqueous solution onto Bael Tree leaf powder. *Journal of Engineering Science and Technology*, 4(4), 351-363.
- Mansur, N. F., Hanafiah, M. A. K. M., & Ismail, M. (2020). Pb(II) Adsorption onto Urea Treated *Leucaena leucocephala* Leaf Powder: Characterization, Kinetics and Isotherm Studies. *Nature Environment and Pollution Technology*, 19(1), 311-318.
- McKay, G. (1982). Adsorption of dyestuffs from aqueous solutions with activated carbon I: Equilibrium and batch contact-time studies. *Journal of Chemical Technology and Biotechnology*, 32(7-12), 759-772.
- Mehdizadeh, S., Sadjadi, S., Ahmadi, S., & Outokesh, M. (2014). Removal of heavy metals from aqueous solution using platinum nanoparticles/zeolite-4A. *Journal of Environmental Health Science and Engineering*, 12(1), 1-7.

- Mor, S., Ravindra, K., De Vissher, A., Dahiya, R. P., & Chandra, A. (2006). Municipal solid waste characterization and its assessment for potential methane generation: A case study. *Science of The Environment*, 371(1-3), 1-10.
- Ngah, W. S. W., & Fatinathan, S. (2010). Adsorption characterization of Pb(II) and Cu(II) ions onto chitosan-tripolyphosphate beads: Kinetic, equilibrium and thermodynamic studies. *Journal of Environmental Management*, 91(4), 958-969.
- Ngaini, Z., Azlin, A. R. K. A., Nazlina, S., Hasnain, H., Norhaizat, S., Teng, J. X., & Lawai, V. (2013). Production of fire-retardant sound-absorbing panels from sago waste. *Journal of Tropical Forest Science*, 25(4), 510-515.
- Ngaini, Z., Wahi, R., Halimatulzahara, D., & Yusoff, N. A. N. M. (2014a). Chemically modified sago waste for oil absorption. *Pertanika Journal of Science & Technology*, 22(1), 153-161.
- Ngaini, Z., Noh, F., & Wahi, R. (2014b). Esterified sago waste for engine oil removal in aqueous environment. *Environmental Technology*, 35(22), 2761-2766.
- Ngaini, Z., Noh, F., & Wahi, R. (2018). Facile sorbent from esterified cellulosic sago waste for engine oil removal in marine environment. *International Journal of Environmental Science and Technology*, 15(2), 341-348.
- Park, J., Hung, I., Gan, Z., Rojas, O. J., Lim, K. H., & Park, S. (2013). Activated carbon from biochar: influence of its physicochemical properties on the sorption characteristics of phenanthrene. *Bioresource Technology*, 149, 383-389.
- Pathania, D., Sharma, S., & Singh, P. (2017). Removal of methylene blue by adsorption onto activated carbon developed from *Ficus carida* bast. *Arabian Journal of Chemistry*, 10, 1445-1451.
- Patil, S., Renukdas, S., & Patel, N. (2011). Removal of methylene blue, a basic dye from aqueous solutions by adsorption using teak tree (*Tectona grandis*) bark powder. *International Journal of Environmental Science*, 1(5), 711-725.
- Perrin, A., Celzard, A., Albiniak, A., Jasienko-Halat, M., Mareche, J. F., & Furdin, G. (2005). NaOH activation of anthracites: Effect of hydroxide content on pore textures of methane storage ability. *Microporous and Mesoporous Materials*, 81(1-3), 31-40.
- Phang, S. M., Miah, M. S., Yeoh, B. G., & Hashim, M. A. (2000). Spirulina cultivation in digested sago starch factory wastewater. *Journal of Applied Phycology*, 12, 395-400.
- Qian, Q., Machida, M., & Tatsumoto, H. (2008). Textural and surface chemical characteristics of activated carbons prepared from cattle manure compost. *Waste Management*, 28(6), 1064-1071.
- Rafiq, M. K., Bachmann, R. T., Rafiq, M. T., Shang, Z., Joseph, S., & Long, R. (2016). Influence of pyrolysis on physico-chemical properties of corn stover (*zea mays L.*) biochar and feasibility for carbon capture and energy balance. *PLoS ONE*, 11(6), 1-17.
- Rajan, Y., Ngaini, Z., & Wahi, R. (2019). Novel adsorbent from sago-grafted silica for removal of methylene blue. *International Journal of Environmental Science and Technology*, 16, 4531-4542.
- Reed, B. E., & Matsumoto, M. R. (1993). Modelling cadmium adsorption by activated carbon using the langmuir and freundlich isotherm expressions. *Separation Science and Technology*, 28(13-14), 2179-2195.

- Ricordel, S., Taha, S., Cisse, I., & Dorange, G. (2001). Heavy metals removal by adsorption onto peanut husks carbon: characterization, kinetic study and modelling. *Separation and Purification Technology*, 24(3), 389-401.
- Hach-Lange (1989). *Water analysis handbook*. Loveland, CO, USA: HACH, Company.
- Ronsse, F., Van, H. S., Dickinson, D., & Prins, W. (2012). Production and characterisation of slow pyrolysis biochar: Influence of feedstock type and pyrolysis conditions. *GCB Bioenergy*, 5(2), 104-115.
- Senthilkumar, S., Varadarajan, P. R., Porkodi, K., & Subbhuraam, C. V. (2005). Adsorption of methylene blue onto jute fiber carbon: kinetics and equilibrium studies. *Journal of Colloid and Interface Science*, 284(1), 78-82.
- Slade, A. H., Thorn, G. J. S., & Dennis, M. A. (2011). The relationship between BOD:N ratio and wastewater treatability in a nitrogen-fixing wastewater treatment system. *Water Science and Technology*, 63(4), 627-632.
- Stella, M. G., Sugumaran, O., Niveditha, S., Ramalakshmi, B., Ravichandran, P., & Seshadri, S. (2016). Production, characterization and evaluation of biochar from pod (*pisum sativum*), leaf (*bassica olerase*) and peel (*citrus sinensis*) wastes. *International Journal of Recycling of Organic Wastes on Agriculture*, 5(1), 43-53.
- Tan, I. A. W., Ahmad, A. L., & Hameed, B. H. (2008). Adsorption of basic dye on high-surface-area activated carbon prepared from coconut husk: Equilibrium, kinetic and thermodynamic studies. *Journal of Hazardous Materials*, 154(1-3), 337-346.
- Tara, N., Siddiqui, S. I., Rathi, G., Chaudhry, S. A., Inamuddin, & Asiri, A. M. (2020). Nano-engineered adsorbent for the removal of dyes from water: A review. *Current Analytical Chemistry*, 16, 14-40.
- Taty-Costodes, V. C., Fauduet, H., Porte, C., & Delacroix, A. (2003). Removal of Cd(II) and Pb(II) ions from aqueous solutions by adsorption onto sawdust *pinus sylvestis*. *Journal of Hazardous Materials*, 105(1-3), 121-142.
- Tsai, W. T., Chang, C. Y., Lin, M. C., Chien, S. F., Sun, H. F., & Hsieh, M. F. (2001). Adsorption of acid dye onto activated carbons prepared from agricultural waste bagasse by ZnCl₂ activation. *Chemosphere*, 45(1), 51-58.
- Wahi, R., & Senghie, H. (2010). The use of microwave derived activated carbon for removal of heavy metal in aqueous solution. *Journal of Science and Technology*, 3(1), 97-108.
- Wahi, R., Chuah, A. L., Nourouzi, M. M., Ngaini, Z., & Choong-Shean-Yaw, T. (2017a). Utilization of esterified sago bark fibre waste for removal of oil from palm oil mill effluent. *Journal of Chemical Engineering*, 5(1), 170-177.
- Wahi, R., Zuhaidi, N. F. Q., Yusof, Y., Jamel, J., Kanakaraju, D., & Ngaini, Z. (2017b). Chemically treated microwave-derived biochar: An overview. *Biomass and Bioenergy*, 107, 411-421.
- Wahi, R., Ngaini, Z., & Jok, V. U. (2009). Removal of mercury, lead and copper from aqueous solution by activated carbon of palm oil empty fruit bunch. *World Applied Sciences Journal*, 5, 84-91.

- Wang, X., Zhu, N., & Yin, B. (2008). Preparation of sludge-based activated carbon and its application in dye wastewater treatment. *Journal of Hazardous Materials*, 153(1-2), 22-27.
- Winkler, M. (2013). *Optimal nutrient ratios for wastewater treatment*. Colorado, USA: Hach Company.
- Yue, C., Li, L. Y., & Johnston, C. (2018). Exploratory study on modification of sludge-based activated carbon for nutrient removal from stormwater runoff. *Journal of Environmental Management*, 226, 37-45.